International Journal of Recent Technology and Engineering (IJRTE)
ISSN: 2277-3878, Volume-8 Issue-4, November 2019

Effect of Torsional Element towards High-Speed Rotating Shaft's Critical Speed at Different Boundary Conditions

Abdul Malek Abdul Wahab, Z A Rasid, H. M. Y. Norfazrina, Ahmad Khushairy Makhtar

Abstract*: Efficiency improvement that can be provided by the high-speed rotating equipment becomes a concern for designers nowadays. Since the high-speed rotating machinery was capable of rotating at very near to critical speed, the accurate estimation of critical speed needs to be considered. This paper investigated the effect of torsional element towards critical speed of high-speed rotating shaft system for pinned-pinned (P-P), clamped-free (C-F) and clamped-free (C-F) boundaries condition. The Nelson's finite element model that considers the torsional effect was developed for formulating the finite element (FE) model. This FE model was used to derive Mathieu-Hill's equation and then solved by applying the Bolotin's theory. From the solution, the Campbell's diagram of the high-speed shaft was plotted. It was found that torsional motion has significant effect on the critical speed for different boundary conditions. The difference between critical speed of 4DOF and 5DOF models can be as high as 6.91 %.

***Index Terms*: boundary conditions, critical speed, high speed, torsional motion.**

I. INTRODUCTION

The high-speed rotating equipment becomes a demand nowadays. The high speed rotating equipment can produce high power output with reduction in size and weight compared to conventionally designed machines [1]. Boglietti *et al*. [2] and Gerada *et al*. [3] classified the high speed of rotating equipment lies in between 10000 RPM and 100000 RPM.

In the rotating shafts condition the gyroscopic momentum has the effect on the critical speed. The first work on the effect of gyroscopic momentum was by Green [4]. He studied the gyroscopic effect on the natural frequency of flexible rotors. Work by Eshleman and Eubanks [5] and Rao [6] also have explored the changes of natural frequency for rotating shafts.

The critical speed can cause whirling condition to rotating shafts or rotor. Whirling motion is known to be the major cause of disturbance that causes the instability conditions and may lead to failure in rotating machine elements. In whirling condition the shaft bow out as the results of the plane of enclosed bent up shaft–axis and the bearing centre line rotate about the bearing centre line [7].

Due to the importance of estimating accurately the critical speed, research on this subject has been done by many researchers. Work by Whalley and Abdul-Ameer [8] calculated the critical speed and rotational frequency of shaft-rotor systems where the shaft profile is contoured. Taplak and Parlak [9] obtained critical speeds, Campbell diagram and the response of the rotor in analyse the dynamic characteristics of a small gas turbine rotor.

Campbell diagram is used to predict the critical speed of the rotating system. It is very important to consider the excitation frequency of external force and the natural frequency of the rotor system at the design stage of the shaft system to avoid any unstable vibration from happening. It is even more important to estimate the critical speed in the high-speed rotating machinery, since the system is capable of rotating at very near to critical speed.

This work investigated the significant effect of torsional element towards the critical speed condition of high-speed rotating shaft system, with different boundaries condition, pinned-pinned (P-P), clamped-free (C-F) and clamped-free (C-F). The focus was on the effect of boundaries condition, P-P, C-F and C-F on the behaviour of critical speed and the vibration frequency of the rotating shaft. The Nelson's finite element model [10] was used to developed the finite element (FE) model. This model considered additional torsional element. The Mathieu-Hill type of equation was derived by applying the Bolotin's method [11]. Then these quadratic eigenvalues problem equation was solved to predict Campbell's diagram, where forward and backward frequencies of the shaft were plotted

II. MATERIALS AND METHODS

Fig. 1 shows the shaft under pinned-pinned condition which is used in this paper. L is the length of the shaft while d is the diameter of the shaft. Ω is the rotating speed of the shaft. The geometry and mechanical properties of the shaft is given in Table-I.

Manuscript published on November 30, 2019.
* Correspondence Author
Abdul Malek Abdul Wahab*, Faculty of Mechanical Engineering Universiti Teknologi MARA, Shah Alam, Selangor, Malaysia. Email: abdmalek@uitm.edu.my
Zainudin A. Rasid, Malaysia-Japan International Institute of Technology (MJIIT), Universiti Teknologi Malaysia Kuala Lumpur, Malaysia. Email: arzainudin.kl@utm.my
Norfazrina Hayati Binti Mohd Yatim, Department of Mechanical Engineering Kulliyah of Engineering International Islamic University Malaysia Kuala Lumpur, Malaysia. Email: norfazrina@iium.edu.my
Ahmad Khushairy Makhtar, Faculty of Mechanical Engineering Universiti Teknologi MARA, Shah Alam, Selangor, Malaysia. Email: ahmadkhushairy@uitm.edu.my

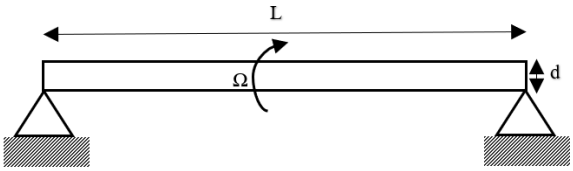

Fig. 1 Rotating shaft under pinned-pinned condition.

Table-I: Geometric and material properties of the rotating shaft for different boundary condition

Young's modulus, E	207 GPa
Modulus of rigidity, G	79.6 GPa
Poisson's ratio, v	0.303
Density, ρ	7833 kg/m^3
Radius, r	round tube with r_{inner} = 0 m, r_{outer} = 0.0508 m
Length, L	1.27 m
Shear factor, κ	0.9
Yield strength, S_y	400 MPa

The total potential energy stored in the beam element that due to bending, and torsional motion is expressed as (1);

$$U = \underbrace{\frac{1}{2}\int_{-a}^{+a} EI_p(\acute{\theta}_z^2 + \acute{\theta}_y^2)\,dx}_{\text{Bending element}} + \underbrace{\frac{1}{2}\int_{-a}^{+a} \kappa GA(\acute{v} - \theta_z)^2 + \kappa GA\left(\acute{w} + \theta_y\right)^2\,dx}_{\text{Shear element}} + \underbrace{\frac{1}{2}\int_{-a}^{+a} GJ\acute{\theta}_x^2\,dx}_{\text{Torsional element}} \quad (1)$$

In order to make the beam element to be in rotating condition, Euler angle transformation was applied [12] to (1). For potential energy, there are no differences arises between static and rotating formulation. Therefore, the total potential energy of rotating beam due to bending and torsional motion is described in (1).

For differential Timoshenko beam element, deflection due to the shear force is important. The shear force (Q) over a linearly approached cross section is proportional with the shear force for material that can be represented as (2);

$$Q = \kappa GA\lambda \quad (2)$$

Where λ is equal to the total of strain element in bending condition. κ is the effective shear factor on the cross sectional that depends on the material properties and cross-sectional shape. In literature [12], [13] the value of κ suggested for rectangular cross section was 5/6 while for circular cross section was 11/13. Meanwhile, A is the cross-sectional area of the shaft.

Equation (3) is the kinetic energy of beam element. The beam is considered to rotate at constant angular velocity Ω about the x-axis and small deformation is neglected. As Euler angle transformation is applied to make the beam in rotating condition [12], the total kinetic energy of rotating beam element in term of bending and torsional condition is derived as (3);

$$T = \underbrace{\frac{1}{2}\int_{-a}^{+a} \rho A((\dot{v})^2 + (\dot{w})^2)\,dx}_{\text{Translation element}} + \underbrace{\frac{1}{2}\int_{-a}^{+a} \rho I_y(\dot{\theta}_y)^2 + \rho I_z(\dot{\theta}_z)^2\,dx}_{\text{Rotary inertia element}} + \underbrace{\int_{-a}^{+a} \rho I_x\theta_z\dot{\theta}_y\,dx\,\Omega}_{\text{Gyroscopic element}} + \underbrace{\frac{1}{2}\int_{-a}^{+a} \rho I_x(\dot{\theta}_x)^2\,dx}_{\text{Torsional element}} \quad (3)$$

In (3) additional gyroscopic effect is raised as Euler angle transformation is applied. The 5DOF FE model was developed with additional torsional element. While 4DOF model was established by using the Timoshenko beam theory without adding any torsional element. The significant outcome of additional torsional element towards whirling speed at high speed was investigated by comparing the two model.

The beam understudy was discretized into several elements where each element consisted of 2 nodes. For the 5DOF model, each node was described by 5 degrees of freedom which were v, w, θ_y, θ_z, and θ_x while for the 4DOF model, each node was represented by 4 degrees of freedom which were v, w, θ_y and θ_z.

In this study, the 5DOF shaft element was explained in Wahab et.al [15]. Mathieu-Hill equation was used to represent the general equation as in (4), where [M], [G], [K] and [K_g] are the elemental mass, gyroscopic, stiffness and geometric stiffness matrices, respectively, P(t) is the periodic axial force, α is the static load factor, β is the dynamic load factor and ϕ is the excitation frequency.

$$[M]\{\ddot{q}\} + \Omega[G]\{\dot{q}\} + ([K] - [K_g](\alpha P^* + \beta P^* \cos\phi T\,(t))\{q\} = 0 \quad (4)$$

The Mathieu-Hill's equation was solved using Bolotin's theory [16][15]. As α = 0, β = 0, ω_0 = ϕ/2 and Ω ≠ 0, the equation for whirling analysis becomes;

$$(\phi^2[M_E] + \phi[G_E] + [K_E])q = 0 \quad (5)$$

where ω_0 is the non-rotating natural frequency of shaft.

III. RESULTS AND DISCUSSION

Free Vibration Analysis

In this study, the conditions of the rotating shaft under P-P, C-F and C-F boundary condition were determined.

For investigating the effect of torsional motion, the critical speed for both models 4DOF and 5DOF were determined at different rotational speeds. Fig. 2 shows the Campbell diagram for the 4DOF and 5DOF models under P-P, C-F and C-F boundary conditions at the first mode. Campbell diagram was plots of forward and backward frequencies on y-axis over a wide shaft speed on x-axis [17]. BF is referring to the backward frequency while FF is referring to the forward frequency as speed of the shaft system increases. Fig. 2 also shows the 1st Engine Order line that represents points where natural frequency is equal to the speed of motor.

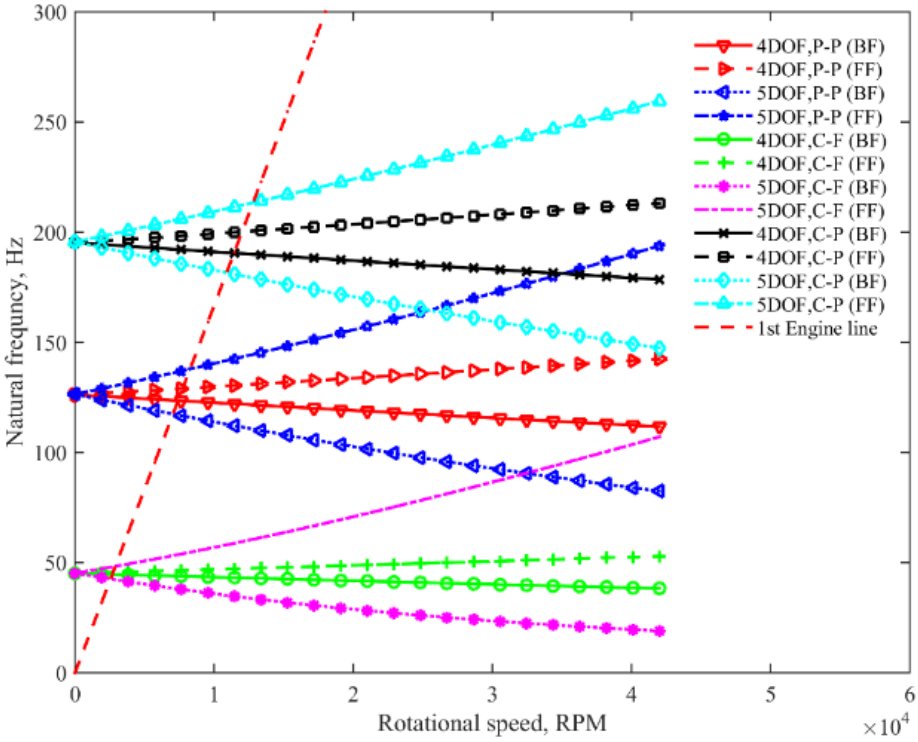

Fig. 2 The whirling speed condition under different boundary conditions at the 1st modes of frequency.

At static condition, the natural frequency changed for different boundary condition as shown in the Fig. 2.

C-P boundary condition showed the highest natural frequencies for both models of 4DOF and 5DOF. Then are followed by the P-P and the C-F boundary conditions. Table-II shows the natural frequency of shaft system at the first mode for C-P, C-F and P-P boundary conditions. C-F boundary condition showed significant effect of torsional motion compare another boundary condition with 2.43 % differences.

Table- II: The first mode natural frequency for 4DOF and 5DOF model under different boundary condition.

Boundary condition	Natural frequency, Hz 4DOF	Natural frequency, Hz 5DOF	Differences (%)
C-P	195.6	194.0	-0.82
P-P	126.4	125.3	-0.87
C-F	45.2	46.3	2.43

More importantly, in all cases of boundary condition, as the rotating speed of the shaft was increased, the BF given by both the 4DOf and 5DOF models droped while the FF increased its frequency values. This result was consistent with what has been stated in literature [18], [19]. This phenomenon was due to the gyroscopic effect that occured in a rotating shaft system. The gyroscopic term is generally written as skew-symmetric matrix which is added to damping element of the shaft system. This skew-symmetric matrix has stiffening and softening effects as speed changes. Consider for the FF mode, the gyroscopic effect increased with the increment of stiffness of the shaft as rotating speed increased and as such the natural frequency increased as well. The effect was reversed for the case of the BF.

The percentage differences between 5DOF and 4DOF for the first mode frequencies is shown in Fig. 3. There were significant different between each boundary conditions, P-P, C-F and C-P as rotating speed increases. C-F boundary condition showed the highest percentage difference in FF and BF direction, followed by P-P boundary conditions. C-P boundary condition showed the lowest differences. These results showed that additional torsional element has significant effect on predicting frequency of rotating shaft for C-F, P-P and C-P boundary conditions especially at high speed.

Table-III compare the critical speed at the first mode for the 4DOF and 5DOF model. The value at rotating speed axis at the intersection point between the straight Engine Order line and frequency is the critical speed of the shaft system in RPM. As explained in literature, the critical speed was the speed at which the shafts tend to vibrate violently in transverse direction due to the occurrences of resonance [8]. From the tables, it can be said that in general the critical speed was varied for different boundary conditions for both modes. The C-P boundary conditions showed the highest critical speed then follows by C-F and P-P for both 4DOF and 5DOF models.

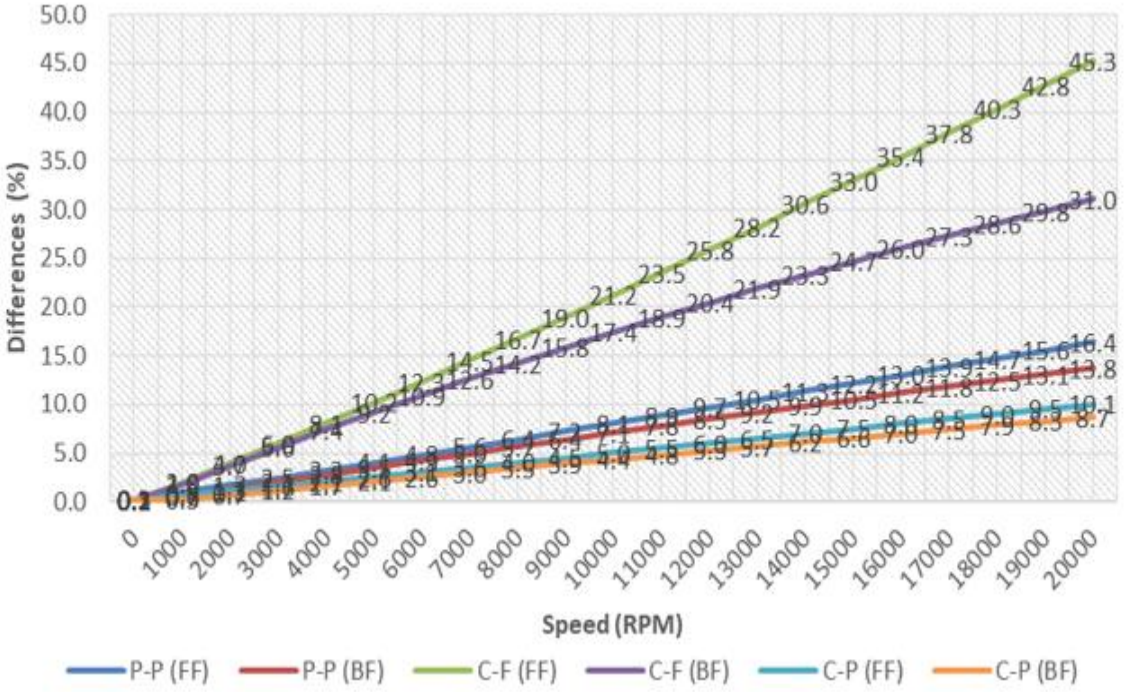

Fig. 3 The first mode percentage differences in frequency corresponds to the 4DOF and 5DOF models for P-P, C-F and C-P boundary conditions as rotating speed rises.

Table- III: The first mode whirling speeds corresponds to the 4DOF and 5DOF models for P-P, C-F and C-P boundary conditions.

Boundary condition	Frequency direction	Critical speed, RPM 4DOF	Critical speed, RPM 5DOF	Differences (%)
P-P	BF	7420	7074	4.66
	FF	7744	8279	6.91
C-F	BF	2683	2559	4.62
	FF	2741	2903	5.91
C-P	BF	11430	10890	4.72
	FF	12010	12810	6.66

Fig. 4 compares the deflection of the shaft for 4DOF and 5DOF model as rotating speed rises for C-F, P-P and C-P boundary conditions. Figure shows that at critical speed condition, the deflection of the shaft is infinity as resonance occurs. In this analysis, the eccentricity gravitational distance of e = 0.02 m was used as the threshold of shaft to show the deflection. Table-IV shows how the speeds associated with the deflection correspond to the 5DOF and 4DOF model differ for C-F, P-P and C-P boundary conditions. Significant effect of torsional motion can highly be identified at C-P boundary condition as the 5DOF model estimated the 0.02 m deflection occurs at 5450 RPM while the 4DOF model predicted it to occur at 5700 RPM, a difference of 250 RPM. For P-P and C-F boundary conditions, the estimation made by the 5DOF model gave 150 RPM and 50 RPM difference compared to those of the 4DOF model respectively. This showed that the 5DOF model can predict the instability of shaft at rotating speed in average 4% different than those of the 4DOF model. This was a significant number since accurate detection of the instability condition can reduce the risk of the shaft system to experience failure.

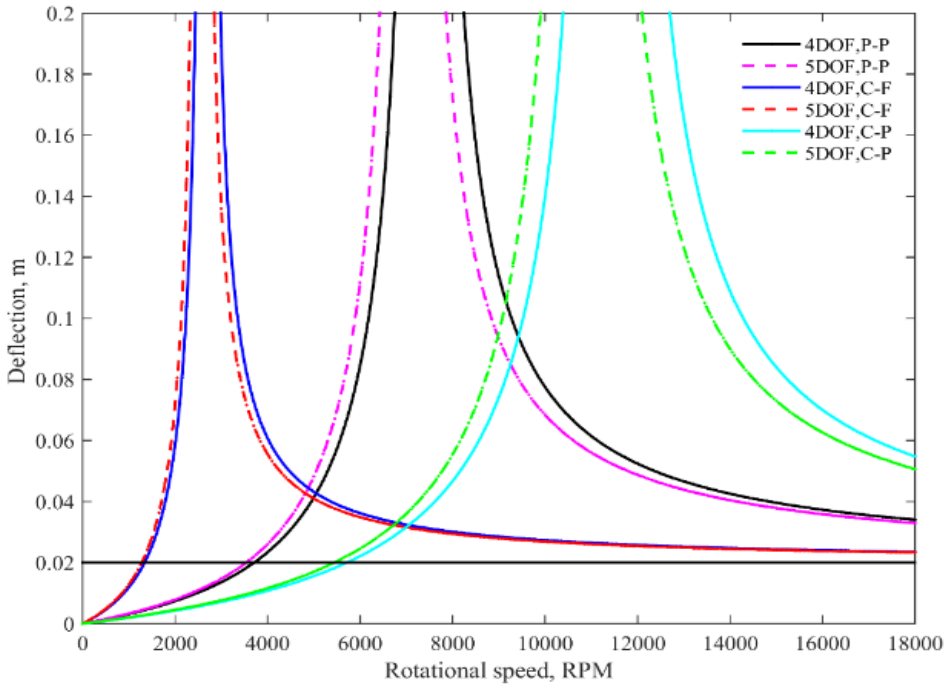

Fig. 4 The comparison of deflection as rotating speed increases for 1st mode pinned-pinned boundary condition.

Table- IV: Comparison of speed for shaft system deflect at 0.02 m.

Boundary condition	Speed, RPM 4DOF	Speed, RPM 5DOF
P-P	3550	3700
C-F	1250	1300
C-P	5450	5700

IV. CONCLUSION

In this work, a FE model of rotating shaft with additional torsional motion element was developed. At the static condition, the torsional element only significant for C-F boundary conditions compare to P-P and C-P. As rotating speed was applied the vibration frequency was separated into two directions of FF and BF due to gyroscopic effect. The separation grows as rotating speed is increased.

The additional torsional element that included in 5DOF models showed significant effect on predicting frequency of rotating shafts under C-F, P-P and C-P boundary conditionsThis is considered that the additional torsional motion is important for modelling the rotating shat at high speed.

ACKNOWLEDGMENT

The authors acknowledge the support in this study from MJIIT, Universiti Teknologi Malaysia and Universiti Teknologi Mara.

REFERENCES

1. H. C. Lahne, O. Moros, and D. Gerling, “Design considerations when developing a 50000 rpm high-speed high-power machine,” *2015 17th Eur. Conf. Power Electron. Appl. EPE-ECCE Eur. 2015*, pp. 1–10, 2015.
2. A. Boglietti, C. Gerada, and A. Cavagnino, “High-speed electrical machines and drives,” *IEEE Trans. Ind. Electron.*, vol. 61, no. 6, pp. 2943–2945, 2014.
3. D. Gerada, A. Mebarki, N. L. Brown, C. Gerada, A. Cavagnino, and A. Boglietti, “High-speed electrical machines: Technologies, trends, and developments,” *IEEE Trans. Ind. Electron.*, vol. 61, no. 6, pp. 2946–2959, 2014.
4. R. Green, “Gyroscopic effects of the critical speeds of flexible rotors,” *J. Appl. Mech*, vol. 15. 1948.
5. R. L. Eshleman and R. A. Eubanks, “On the Critical Speeds of a Continuous Shaft-Disk System,” *J. Manuf. Sci. Eng.*, vol. 89, no. 4, pp. 645–652, Nov. 1967.
6. J. S. Rao, “Finite Element Methods for Rotor Dynamics,” in *History of Rotating Machinery Dynamics SE - 16*, vol. 20, Springer Netherlands, 2011, pp. 269–297.
7. A. G. Ambekar, *Mechanical Vibrations and Noise Engineering*. PHI Learning, 2006.
8. R. Whalley, M. Ebrahimi, and A. Abdul-Ameer, “High-speed rotor-shaft systems and whirling identification,” *Proc. Inst. Mech. Eng. Part C-Journal Mech. Eng. Sci.*, vol. 221, no. 6, pp. 661–676, 2007.
9. H. Taplak and M. Parlak, “Evaluation of gas turbine rotor dynamic analysis using the finite element method,” *Measurement*, vol. 45, no. 5, pp. 1089–1097, Jun. 2012.
10. E. S. Zorzi and H. D. Nelson, “The Dynamics of Rotor-Bearing Systems With Axial Torque—A Finite Element Approach,” *J. Mech. Des.*, vol. 102, no. 1, p. 158, 1980.
11. V. V. Bolotin, “THE DYNAMIC STABILITY OF ELASTIC SYSTEMS. VOLUME 2,” DTIC Document, 1962.
12. F. Raffa and F. Vatta, “Gyroscopic effects analysis in the Lagrangian formulation of rotating beams,” *Meccanica*, pp. 357–366, 1999.
13. J. R. Hutchinson, “Shear Coefficients for Timoshenko Beam Theory,” *J. Appl. Mech.*, vol. 68, no. 1, pp. 87–92, 2001.
14. G. R. Cowper, “The shear coefficient in Timoshenko’s beam,” *Trans. ASME J. Appl. Mech.*, vol. 33, no. 4, pp. 335–340, 1966.
15. [15] N. F. M. N. Wahab, A.M.A., Yusof, Z., Rasid, Z.A., Abu, A., Rudin, “Dynamic Instability of High-Speed Rotating Shaft with Torsional Effect,” *Int. J. Automot. Mech. Eng.*, vol. 15, no. 4, pp. 6034–6051, 2018.
16. V. V. Bolotin, “The Dynamic Stability of Elastic Systems,” *Am. J. Phys.*, vol. 33, no. 9, p. 752, 1965.
17. E. Swanson, C. D. Powell, and S. Weissman, “A practical review of rotating machinery critical speeds and modes,” *Sound Vib.*, vol. 39, no. May, pp. 10–17, 2005.

18. G. Sauer and M. Wolf, "Finite element analysis of gyroscopic effects," *Finite Elem. Anal. Des.*, vol. 5, no. 2, pp. 131–140, Jul. 1989.
19. B. G. Bazehhour, S. M. Mousavi, and A. Farshidianfar, "Free vibration of high-speed rotating Timoshenko shaft with various boundary conditions: effect of centrifugally induced axial force," *Arch. Appl. Mech.*, vol. 84, no. 12, pp. 1691–1700, Dec. 2014.

AUTHORS PROFILE

Dr. Abdul Malek is a Senior Lecturer in Faculty of Mechanical Engineering in Universiti Teknologi Mara, Shah Alam.. He received her doctorate in Dynamics Structure from Universiti Teknologi Malaysia (UTM), Malaysia. Dr. Abdul Malek has several research publications in well-known international Journals and conferences. His research interests include the parametric excitation condition and instability in high speed rotating machine.

Dr. Zainudin is a Senior Lecturer of Mechanical Engineering, Malaysia-Japan International Institute of Technology, Universiti Teknologi Malaysia (UTM), Malaysia. He received her doctorate in Aerospace Engineering from Universiti Putra Malaysia (UPM), Malaysia. Dr. Zainudin has several research publications in well-known international Journals and conferences. His research interests include the composite material and carbon nanotube.

Dr. Norfazrina Hayati is an Assistant Professor in Kulliyyah of Engineering, International Islamic University Malaysia, Gombak Campus, Malaysia. She received her doctorate in Dynamics Structure from Universiti Teknologi Malaysia (UTM), Malaysia. Dr. Norfazrina Hayati has several research publications in well-known international Journals and conferences. His research interests include the mechanical systems engineering.

Dr. Ahmad Khushairy Makhtar is a Senior Lecturer in Faculty of Mechanical Engineering in Universiti Teknologi Mara, Shah Alam. He received his doctorate in Risk Engineering from University of Tsukuba, Japan. Dr. Ahmad Khushairy has several research publications in well-known international Journals and conferences. His research interests include about human factors and ergonomics, human responds to vibration, Risk Analysis and measurements etc.